Radiative Constraints on the Hydrological Cycle in an Idealized Radiative–Convective Equilibrium Model

KEN TAKAHASHI

Atmospheric and Oceanic Sciences Program, Princeton University, Princeton, New Jersey

(Manuscript received 31 March 2008, in final form 17 June 2008)

ABSTRACT

The radiative constraints on the partitioning of the surface energy budget and, hence, on the strength of the hydrological cycle are analyzed in an idealized one-dimensional radiative–convective equilibrium model formulated in terms of the energy budgets at the top of the atmosphere, the subcloud layer, and the free atmosphere, which enables it to predict both surface relative humidity and the air–sea temperature difference. Using semigray radiative transfer, a semianalytical solution was obtained that explicitly shows how the surface latent heat flux (LHF) is related to the radiative properties of the atmosphere. This solution was also used in conjunction with a full radiative transfer code and was found to provide reasonably realistic quantitative estimates.

In the model the LHF is fundamentally constrained by the net longwave flux divergence above the level of condensation by lifting (LCL) and by the atmospheric absorption of shortwave radiation, with only a weak indirect control by near-surface moisture. The latter implies that the Clausius–Clapeyron relation does not directly constrain the strength of the hydrological cycle. Under radiative perturbations, the changes in LHF are determined by the changes in the net longwave fluxes at the LCL, associated mainly with the changes in the longwave transmissivity, and by the changes in shortwave absorption by the atmosphere (e.g., by increased water vapor).

Using a full radiative transfer model with interactive water vapor feedback with the semianalytical solution indicates a rate of change in LHF with greenhouse forcing of around 2 W m^{-2} K^{-1} of surface warming, which corresponds to the Planck feedback ($\sim$3.2 W m^{-2} K^{-1}) multiplied by a coefficient of order one that, to first approximation, depends only on the relative magnitudes of the net longwave radiation fluxes at the LCL and the top of the atmosphere (i.e., on the shape of the vertical profile of the net longwave flux).

1. Introduction

The question of how the hydrological cycle will change in the context of global climate change is of considerable societal and scientific interest. One fundamental aspect of this cycle is its global mean (i.e., global mean surface evaporation and precipitation), which is intrinsically tied to the global atmospheric and surface energy budgets (Allen and Ingram 2002, hereafter AI02). Although the global average of the hydrological cycle does not have as much practical importance as its regional manifestations, it is a fundamental aspect of climate and a quantitative and predictive theory for it would provide guidance for the diagnosis of biases in climate models, help to sort out possible discrepancies with observational estimates (e.g., Wentz et al. 2007), and help the interpretation of model simulations of climate regimes significantly different from the present one (e.g., AI02; Held and Soden 2006, hereafter HS06).

Comprehensive climate models project an increase in the global-mean atmospheric moisture content associated with global warming that is well explained by the changes in the saturation specific humidity, which is a strong function of temperature, for constant relative humidity (HS06). The global mean hydrological cycle also increases, but at a smaller percentage rate than moisture (AI02; HS06), which indicates that the residence time of water vapor also increases with the warming, which in turn can be interpreted as a slowing down of the motions that transport moisture vertically (Betts 1998; HS06; Vecchi and Soden 2007). However, a mechanistic theory for the changes in the residence time (or in moisture-transporting motions) based on

Corresponding author address: Ken Takahashi, NOAA/Geophysical Fluid Dynamics Laboratory, 201 Forrestal Rd., Princeton, NJ 08540–6649.
E-mail: ken.takahashi@noaa.gov

DOI: 10.1175/2008JAS2797.1

moist dynamics is lacking, so it is not possible at present to predict the changes in *both* the global hydrological cycle and the residence time given the changes in moisture from this perspective.

Another approach considers the global hydrological cycle in the context of the global energy budget of the troposphere (AI02). This brings the complex physics of radiative transfer into the problem, which makes it difficult to produce a simple conceptual theory; so, for example, AI02 take an empirical approach by which the behavior of the radiative fluxes is fit to observed (or modeled) changes in temperature, and changes in the sensible heat fluxes (SHFs) are neglected. One of the main difficulties with a theoretical approach based on the radiative transfer physics is the great complexity in the detailed interactions between radiation at different wavelengths and the atmospheric gases. However, to the extent that these complexities are not essential for understanding the qualitative relation between the net radiative energy fluxes and the surface energy budget, realism in the radiative transfer can be sacrificed in a favor of a less realistic but theoretically simpler representation of the radiative physics. For example, the semigray approximation, in which the atmosphere is assumed to be transparent to shortwave radiation and the longwave emissivities of greenhouse gases are independent of frequency, makes the problem mathematically tractable and exact solutions might be found in some cases (e.g., Goody and Yung 1989; Weaver and Ramanathan 1995).

Another simplifying approximation is to consider a radiative–convective equilibrium model in which large-scale horizontal dynamics (e.g., associated with differential heating and rotation) are ignored. This type of model has been successful in improving our understanding of the processes controlling the vertical thermal structure of the atmosphere and its sensitivity to radiative perturbations (see Ramanathan and Coakley 1978 for a review), as well as providing insights into tropical climate (e.g., Sarachik 1978; Betts and Ridgway 1989, hereafter BR89). Although it is not obvious that this is an adequate approximation for a differentially heated rotating planet [however, there is some evidence that it might be; see O'Gorman and Schneider (2007), hereafter OS07)], the understanding of this simpler system is likely a prerequisite to understanding the general case.

In this study, these two approaches are combined into an idealized radiative–convective equilibrium model with semigray radiation transfer (described in section 2), which is exposed to a wide range of longwave ("greenhouse") forcings (section 3). After some simplifying assumptions, this approach succeeds in providing concrete constraints based on the assumed radiative physics, which are expressed in a semianalytical solution (section 4). This solution is then used in combination with a full radiative transfer model to explore the quantitative predictions in a more realistic setting (section 5). The implications of the results, including a comparison to previous similar studies, are discussed in section 6. The last section summarizes the main results and conclusions.

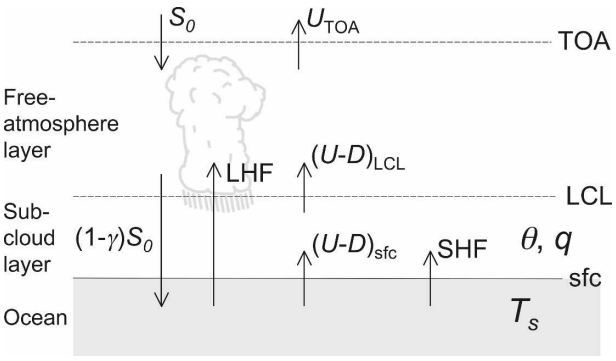

FIG. 1. Schematic diagram indicating the main variables, vertical layers, and energy fluxes considered in the model.

2. Radiative–convective equilibrium model

The model (see Fig. 1 for a schematic depiction) consists conceptually in a hydrostatic atmosphere featuring large-scale subsidence everywhere except for a very small fraction of the area in which strong ascent associated with deep moist convection takes place and from which the latent heating is assumed to be efficiently communicated elsewhere (e.g., Sarachik 1978). In the vertical direction, there is a well-mixed subcloud layer, in which potential temperature θ and specific humidity q are uniform (no special treatment is given to the surface layer), overlying an ocean with surface temperature T_s and a free atmosphere with a thermal structure set everywhere to a pseudoadiabat by deep convection (or, alternatively, the lapse rate may be prescribed). There is no stratosphere in this model. Surface pressure p_0 is fixed to the value of 1000 hPa. A list of the model parameters and their reference values is provided in Table 1.

The design of this model was guided by the following principles: On the one hand, we avoided making strong assumptions about factors that directly affect the surface energy fluxes and that therefore should be part of the solution (e.g., prescribing the surface relative humidity, the air–sea temperature difference, or the

TABLE 1. Constants and parameters with their reference values. The upper block contains physical constants; the lower block contains prescribed model parameters.

Symbol	Parameter	Standard value
c_p	Specific heat at constant pressure	1004 J K^{-1} kg^{-1}
R_d	Dry air constant	287 J K^{-1} kg^{-1}
R_v	Water vapor constant	461 J K^{-1} kg^{-1}
L_v	Enthalpy of vaporization	2.5×10^6 J kg^{-1}
g	Gravitational acceleration	9.8 m s^{-2}
τ_0	Atmospheric longwave optical depth	6
n	Exponent in the formula for the longwave optical depth	4
C	Surface sensible heat and moisture transfer coefficient	10^{-2} kg m^{-2} s^{-1}
S_0	Net shortwave incident at the TOA	240 W m^{-2}
γ	Fraction of S_0 absorbed in the atmosphere	0.29
p_0	Surface pressure	10^5 Pa
Γ	Prescribed free tropospheric lapse rate	6.5×10^{-3} K m^{-1}

Bowen ratio). On the other hand, we made enough simplifications that the system can be well understood, but only when these are supported by observations, so that the model remains qualitatively similar to the earth system for the intended purposes. Because this model is not intended to shed light on climate sensitivity (i.e., changes in θ), this model does not explicitly address changes in clouds, in contrast to other studies with similar models (e.g., Pierrehumbert 1995; Larson et al. 1999). Although there is a possibility that clouds may have a radiative effect relevant to the problem at hand, the issue is so complex that it is left open for future research. The cloud radiative effects are therefore either taken as given or ignored altogether. Physically, the present model is similar to the tropical model of BR89 but with the advantage of having a tractable longwave radiative transfer scheme and other simplifications that greatly ease the analysis.

a. Temperature profile

Given the values of θ and q, the vertical profile of temperature can be determined and used to calculate the longwave fluxes.

In the subcloud layer, extending from the surface to the level of condensation by lifting (LCL), the lapse rate is dry adiabatic. The pressure and temperature at the LCL (p_{LCL} and T_{LCL}, respectively) is determined from the values of θ and q or, alternatively, the physical dependence of p_{LCL} on θ and q is severed and its value is prescribed for the purpose of determining the thermal structure of the atmosphere.

Starting at the LCL, the free atmospheric temperature can be determined either by integrating upward following a pseudoadiabat or, alternatively, by prescribing the lapse rate Γ.

b. Energy budget at the top of the atmosphere

The outgoing longwave flux (U_{TOA}) at the top of the atmosphere (TOA; at $p = 0$) is required to balance the net shortwave radiative flux (S_0) absorbed by the climate system:

$$U_{\mathrm{TOA}} = S_0. \tag{1}$$

To the extent that the atmosphere is optically thick in the longwave range, the surface air temperature θ is closely constrained by this requirement, to the extent that the relation between U_{TOA} and θ is known.

c. Free atmosphere energy budget

The energy budget for the free atmosphere, extending from the LCL to the TOA, yields the latent heat flux (LHF) plus the absorbed shortwave radiation (γS_0, where γ is the prescribed fraction of S_0 absorbed by the free atmosphere) by requiring them to balance the longwave radiative cooling:

$$\mathrm{LHF} + \gamma S_0 = U_{\mathrm{TOA}} - U_{\mathrm{LCL}} + D_{\mathrm{LCL}}, \tag{2}$$

where U and D stand for the net upward and downward longwave fluxes, respectively.

The LHF through the LCL is equal to that at the surface because all of the latent heat is assumed to be released above the LCL (i.e., there is no net condensation in the subcloud layer). The LHF is related to moisture through a bulk formula for surface evaporation:

$$\mathrm{LHF} = L_v C[q_s(T_s) - q], \tag{3}$$

where C is a prescribed effective transfer coefficient that physically depends on wind speed, stability, and air density. This equation allows q to be determined if LHF and T_s are known.

The entrainment flux of sensible heat across the LCL could be parameterized to be proportional to the surface sensible heat flux (Betts 1973; BR89). This entrainment term is, however, typically an order of magnitude smaller than the latent heating, and sensitivity tests show that it only leads to small quantitative differences in the results, so it is neglected in the present model.

Large-scale vertical transports of sensible heat through the LCL are also neglected. On the earth, the net vertical heat transport by large-scale circulations (e.g., Hadley circulation, midlatitude eddies) is approxi-

mately an order of magnitude smaller than the latent heat flux, so this approximation is adequate even in the presence of large-scale transport processes not considered in the radiative-equilibrium framework.

d. Subcloud layer energy budget

The energy budget for the subcloud layer (neglecting entrainment through the LCL) is

$$c_p C \delta T = U_{\mathrm{LCL}} - D_{\mathrm{LCL}} - U_{\mathrm{sfc}} + D_{\mathrm{sfc}}. \quad (4)$$

The term on the lhs is the bulk formula approximation for SHF, where $\delta T \equiv T_s - \theta$ and the effective transfer coefficient C is assumed to be equal to that for moisture. As shown later, this equation constrains δT. The absorption of shortwave radiation in this layer is neglected, which is a convenient but not critical approximation.

e. Longwave radiation

The radiative transfer equations for a semigray atmosphere determine the upward and downward longwave fluxes (U and D, respectively):

$$\frac{dU}{d\tau} = U - \pi B, \quad (5)$$

$$\frac{dD}{d\tau} = \pi B - D, \quad (6)$$

where $\pi B = \sigma T^4$, with T representing the atmospheric temperature profile. The optical depth (including the diffusivity factor) τ is prescribed as a function of pressure p alone as

$$\tau = \tau_0 \left(\frac{p}{p_0} \right)^n, \quad (7)$$

where the exponent n is taken to be 4, based on the fact that the scale height for air density is 4 times larger than that of water vapor (e.g., Goody and Yung 1989; Weaver and Ramanathan 1995; Frierson et al. 2006). Although pressure broadening might be expected to increase the exponent to $n = 5$ (Weaver and Ramanathan 1995), this does not affect the qualitative behavior of the model, so $n = 4$ is used to allow the comparison with the results from OS07.

3. Experiments

The model was run for values of τ_0 ranging from 1.5 to 500, with uniform intervals in log τ_0. The equilibrium state was obtained by allowing a time-dependent version of the system (2)–(7) (providing the ocean and subcloud layers with finite heat capacities) to evolve in time until an effectively steady state was achieved (no evidence for multiple equilibria was found). In this set

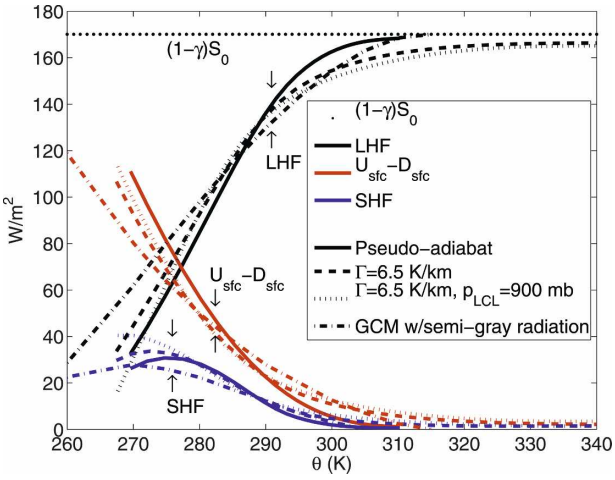

FIG. 2. Surface net shortwave [$(1 - \gamma)S_0$; black dotted], latent heat (LHF; black), longwave ($U_{\mathrm{sfc}} - D_{\mathrm{sfc}}$; red) and sensible heat (SHF; blue) fluxes (W m^{-2}) against surface air temperature (θ; K) as τ_0 is varied. Results are shown for the runs with a pseudoadiabatic profile (solid), $\Gamma = 6.5$ K km^{-1} (dashed), and $\Gamma = 6.5$ K km^{-1} with $p_{\mathrm{LCL}} = 900$ hPa (short dashed), and from a GCM with semigray radiation (dotted–dashed; adapted from Fig. 3 of OS07).

of experiments, the temperature profile in the free atmosphere followed pseudoadiabats. The pressure at the LCL (p_{LCL}) was calculated interactively from the values of θ and q. These experiments can be interpreted as equilibrium climate change runs under greenhouse gas forcing in which the radiative effect of water vapor is not interactive. As τ_0 (i.e., greenhouse gas concentration) increases, the surface air temperature θ increases monotonically (in these experiments, θ ranges from ~270 to 310 K). For the purpose of providing a quantitative description of some results, a reference state corresponding to $\theta = 288$ K (close to the global mean temperature on the earth and corresponding, in this model, to $\tau_0 = 6$) was selected. Around this reference state, a unit change in τ_0 approximately results in a change in θ of around 1.8 K, but more generally θ scales roughly with the logarithm of τ_0, although the sensitivity decreases at higher τ_0 (not shown).

The surface energy fluxes plotted against θ exhibit behavior very similar to the results from a general circulation model (GCM) with semigray radiation reported by OS07 (Fig. 2). Particularly, LHF increases rather linearly with θ for states colder than the reference temperature of 288 K. For higher θ, LHF approaches the surface insolation $(1 - \gamma)S_0$. Consistent with this, the sum of SHF and surface longwave fluxes approaches zero. However, the changes with θ of both of these fluxes are significant, as noted by OS07, so SHF cannot be neglected in principle, as suggested by AI02, for estimating the changes in LHF. The subcloud

layer energy budget (4) indicates that the longwave fluxes through the LCL are also going to zero. It will be shown in the next section that this is the key constraint on LHF as τ_0 is varied.

With semigray radiation, the decrease in longwave fluxes at the LCL could be a direct response to changes in τ_0, which change the radiative transfer between different atmospheric levels. It could also be a result of the change in the lapse rate in the free atmosphere because, as the climate warms, the upper troposphere becomes warmer relative to the surface, and this could lead to a reduction in the upward flux through the LCL. Alternatively, because the net longwave flux typically increases with height, an increase in p_{LCL} toward p_0 as the surface humidity increases would lead to a reduction in the fluxes at this level.

The latter two possibilities can be assessed in a straightforward way in this model. First, the experiments are repeated with the lapse rate Γ in the free atmosphere fixed at the value of 6.5 K km^{-1}. Because this eliminates the negative lapse-rate feedback, the range in θ is much higher for the same values of τ_0 than with the pseudoadiabat. On the other hand, the relation between the energy fluxes and τ_0 is changed very little (not shown), but because the temperature axis is "stretched," smaller slopes result in Fig. 2. This is evidence that the relation between θ and the surface energy fluxes (including the hydrological cycle) result mostly from individual dependencies on the radiative properties of the atmosphere rather than from a direct physical connection between them. In fact, the expected direct effect of warming would be an enhancement of the longwave flux through the LCL and, therefore, a *reduction* in LHF (see section 4a).

In a third set of experiments, the fixed lapse rate is retained and in addition p_{LCL} is prescribed to 900 hPa. The resulting relation between the surface energy fluxes and θ is similar to the second set of experiments (Fig. 2), despite significant variations in p_{LCL} in both of the previous sets of runs.[1] However, although the overall qualitative behavior was unchanged, the quantitative differences are not negligible. For instance, an interactive p_{LCL} results in a slope of LHF with θ about 30% larger near the reference state.

4. Semianalytical solution

As shown in the previous section, the variations in p_{LCL} and Γ, which are the only way by which q directly affects the radiative fluxes in this model, do not affect the overall qualitative behavior of the surface fluxes relative to surface air temperature.

Here these variations are explicitly neglected and the values of p_{LCL} and Γ are prescribed, so the temperature profile and, therefore, the longwave fluxes are decoupled from q, which can be diagnosed from (3) once LHF and T_s are determined. In this way, the hydrological cycle becomes explicitly independent of the details of the moist processes and the system consists now basically in three unknowns (θ, T_s, and LHF), for which there are three equations from the energy budgets [(1), (2), and (4)], as well as the radiative transfer equations [(5) and (6)]. The critical step for finding a solution to the system is determining the longwave fluxes as a function of the model parameters and independent variables without having to solve the radiative transfer equations numerically every time. Fortunately, the semigray radiation scheme allows for this to be overcome to a large extent, as shown next.

Under hydrostatic balance and for a constant lapse rate Γ, the temperature profile is given by $T = \theta(p/p_0)^{R_d\Gamma/g}$. Allowing for a dry adiabatic lapse rate in the subcloud layer, the atmospheric blackbody flux density profile is given by

$$\pi B = \sigma\theta^4 \times \begin{cases} \left(\dfrac{p}{p_0}\right)^{4R_d/c_p} & \text{for} \quad p \geq p_{\mathrm{LCL}}, \\ \left(\dfrac{p_{\mathrm{LCL}}}{p_0}\right)^{4R_d/c_p}\left(\dfrac{p}{p_{\mathrm{LCL}}}\right)^{4R_d\Gamma/g} & \text{for} \quad p < p_{\mathrm{LCL}}. \end{cases} \tag{8}$$

The vertical distribution (in p coordinates) of πB normalized by $\sigma\theta^4$ is fixed and determined by the values of Γ and p_{LCL}. Because p and τ are uniquely related through (7) for a given set of parameters, (8) can be directly substituted into the semigray longwave radiation Eqs. (5) and (6) and, with the approximation $\delta T \ll \theta$, the solution for the net upward longwave flux has the form

$$U - D \approx e^{-\tau_0[1-(p/p_0)^n]}4\sigma\theta^3\delta T + \varepsilon(p; \tau_0, p_{\mathrm{LCL}}, \Gamma)\sigma\theta^4. \tag{9}$$

Here, ε gives the profile of the net longwave flux, normalized by $\sigma\theta^4$, that would result if the surface emitted at the same temperature θ as the surface air (Fig. 3), and the first term on the rhs is the correction that arises from the temperature difference δT. The ε profiles can be determined by prescribing values for Γ and p_{LCL},

[1] Note that p_{LCL} decreases from ~940 hPa near θ = 270 K to ~900 hPa near the reference state and then approaches p_0 as temperature increased further ($p_{\mathrm{LCL}} > 990$ hPa for $\theta > 340$ K).

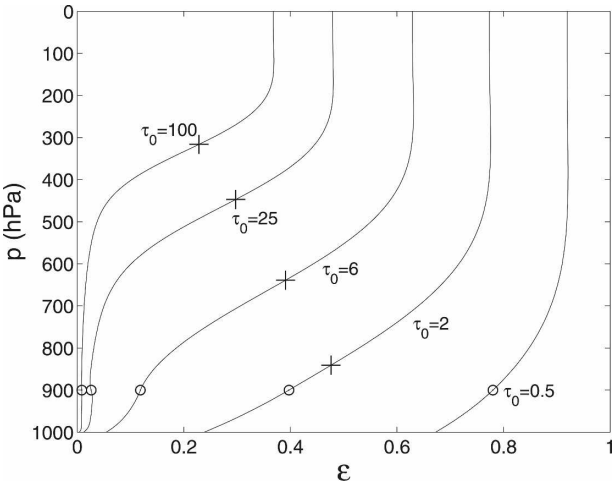

FIG. 3. Normalized vertical profiles of net upward LW fluxes $\varepsilon(p, \tau_0, p_{\mathrm{LCL}}, \Gamma)$ for different values of τ_0, with $\Gamma = 6.5$ K km^{-1}, $p_{\mathrm{LCL}} = 900$ hPa (indicated with circles) and assuming $T_s = \theta$. The levels at which $\tau = 1$ are indicated with crosses.

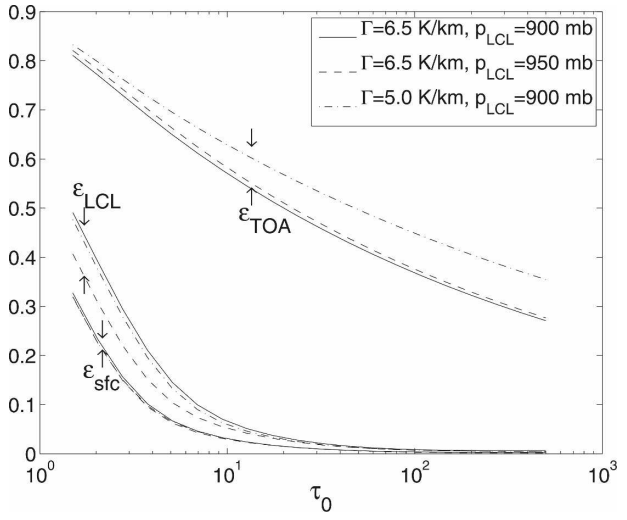

FIG. 4. Normalized net upward LW fluxes (for $T_s = \theta$) at the surface ($\varepsilon_{\mathrm{sfc}}$), LCL($\varepsilon_{\mathrm{LCL}}$), and TOA($\varepsilon_{\mathrm{TOA}}$) as a function of τ_0, for $\Gamma = 6.5$ K km^{-1} and $p_{\mathrm{LCL}} = 900$ hPa (solid), $\Gamma = 6.5$ K km^{-1} and $p_{\mathrm{LCL}} = 950$ hPa (dashed), and $\Gamma = 5$ K km^{-1} and $p_{\mathrm{LCL}} = 900$ hPa (dotted–dashed).

setting $T_s = \theta = \sigma^{-1/4}$ and numerically solving the semigray radiation transfer Eqs. (5) and (6) for $\varepsilon = U - D$. Equation (9) is the key simplification that allows this model to be analytically tractable because it allows the effects of θ and δT on the longwave fluxes to be cleanly separated from those associated with changes in the radiative transfer properties of the atmosphere (e.g., τ_0). In the current setup, with fixed Γ and p_{LCL}, once the ε profiles are determined as a function of τ_0, the system can be immediately solved, even as the other parameters are varied.

The values of ε decrease toward the surface (Fig. 3), implying a flux divergence and therefore cooling. This is because the lapse rate chosen is smaller than the one corresponding to pure radiative equilibrium and therefore requires convective heating for its maintenance (Manabe and Strickler 1964). As τ_0 is increased, the divergence (cooling) is centered at progressively lower pressures, following the level where $\tau = 1$ (Fig. 3). In the layer beneath, the increase in optical thickness with τ_0 is faster because the optical thickness per unit mass ($gd\tau/dp$) is highest near the surface (7). In this layer, as τ_0 increases and the transmission of longwave fluxes becomes very limited, the values of U and D both approach the local blackbody flux πB, so both $U - D$ and $d(U - D)/d\tau$ [from (5) and (6)] become small. Near the surface, however, $\delta T \neq 0$ can maintain a finite $U - D$.

For a sufficiently optically thick subcloud layer, the transmission of the δT correction to the longwave flux emitted by the surface through the LCL and TOA in (9) is relatively small, so we have approximately

$$U_{\mathrm{sfc}} - D_{\mathrm{sfc}} \approx \varepsilon_{\mathrm{sfc}}\sigma\theta^4 + 4\sigma\theta^3\delta T, \tag{10}$$

$$U_{\mathrm{LCL}} - D_{\mathrm{LCL}} \approx \varepsilon_{\mathrm{LCL}}\sigma\theta^4, \quad \text{and} \tag{11}$$

$$U_{\mathrm{TOA}} \approx \varepsilon_{\mathrm{TOA}}\sigma\theta^4, \tag{12}$$

where

$$\varepsilon_{\mathrm{TOA}} \equiv \varepsilon(p = 0; \tau_0, p_{\mathrm{LCL}}, \Gamma), \tag{13}$$

$$\varepsilon_{\mathrm{LCL}} \equiv \varepsilon(p = p_{\mathrm{LCL}}; \tau_0, p_{\mathrm{LCL}}, \Gamma), \quad \text{and} \tag{14}$$

$$\varepsilon_{\mathrm{sfc}} \equiv \varepsilon(p = p_0; \tau_0, p_{\mathrm{LCL}}, \Gamma). \tag{15}$$

The values of $\varepsilon_{\mathrm{LCL}}$ and $\varepsilon_{\mathrm{sfc}}$ rapidly decrease with $\log \tau_0$ (Fig. 4), with the latter always smaller than the former. At the TOA, ε also decreases with $\log \tau_0$ (Fig. 4), but at a slower and more uniform rate. The values of ε at these three levels [(13)–(15)] shown in Fig. 4 completely characterize the semigray radiative transfer scheme for the idealized radiative–convective equilibrium model.

From the energy budgets (1), (2), and (4), using the longwave fluxes (10)–(12), the following solution is obtained:

$$\theta = \left(\frac{S_0}{\varepsilon_{\mathrm{TOA}}\sigma}\right)^{1/4}, \tag{16}$$

$$\delta T = \frac{S_0}{\varepsilon_{\mathrm{TOA}}}\left[\frac{\varepsilon_{\mathrm{LCL}} - \varepsilon_{\mathrm{sfc}}}{4\sigma^{1/4}(S_0/\varepsilon_{\mathrm{TOA}})^{3/4} + c_p C}\right], \quad \text{and} \tag{17}$$

$$\mathrm{LHF} = S_0\left(1 - \gamma - \frac{\varepsilon_{\mathrm{LCL}}}{\varepsilon_{\mathrm{TOA}}}\right). \tag{18}$$

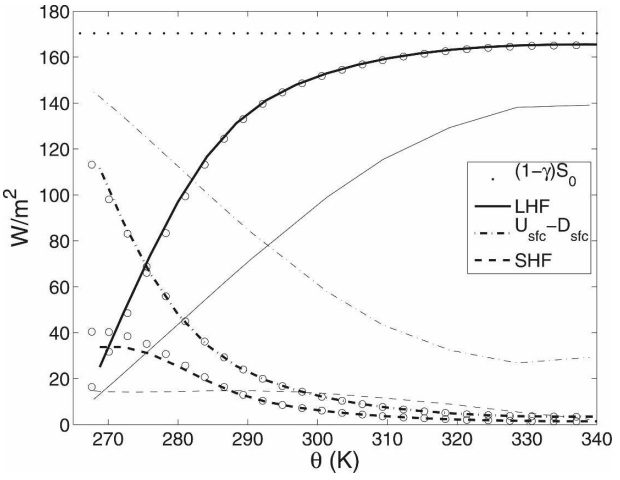

FIG. 5. Semianalytic solution for surface latent (solid), net longwave (dotted–dashed), and sensible (dashed) heat fluxes vs surface air temperature using the semigray radiation for different values of τ_0 (thick lines; the circles indicate results from the full model) and full radiative transfer with interactive water vapor feedback for different concentrations of CO_2 (thin lines). Both models have $\Gamma = 6.5$ K km^{-1} and $p_{\mathrm{LCL}} = 900$ hPa.

This solution is a very good approximation to the full model with fixed Γ and p_{LCL} (Fig. 5), with the best agreement found for values of τ_0 near the reference state and higher, as expected.

Equation (18) expresses the requirement that the net energy flux through the LCL be zero, so the net downward shortwave flux $(1 - \gamma)S_0$ will be balanced by LHF and $(U - D)_{\mathrm{LCL}}$. Because $\varepsilon_{\mathrm{TOA}}$ and, for realistic (positive) tropospheric lapse rates, $\varepsilon_{\mathrm{LCL}}$ are both ≥ 0, then (18) indicates that

$$\mathrm{LHF} \leq (1 - \gamma)S_0. \tag{19}$$

This upper bound on LHF exists because shortwave radiation is the only downward energy flux considered in this model, so it constrains the sum of all of the upward fluxes, including LHF. Exceptions to this might be provided by strong entrainment into the subcloud layer or by a net downward longwave flux through the LCL associated with negative lapse rates.

The sea–air temperature difference δT is constrained to be positive to the extent that $\varepsilon_{\mathrm{LCL}} > \varepsilon_{\mathrm{sfc}}$ (17), which results from the radiative equilibrium lapse rate being larger than the dry adiabatic (Weaver and Ramanathan 1995). Thus, in this model the surface sensible heat flux is always upward to balance the longwave radiative cooling in the subcloud layer (BR89). However, even in the limit of a vanishing C, (17) predicts that δT would only increase by at most a factor of 3 (for the reference climate state) because the longwave fluxes play a significant role in maintaining a small δT.

a. Response to radiative perturbations

For a small radiative perturbation ΔF at the TOA, the response in surface air temperature is given by (16) as

$$\frac{\Delta\theta}{\Delta F} = \frac{1}{4\varepsilon_{\mathrm{TOA}}\sigma\theta^3} \equiv \lambda_0, \tag{20}$$

where λ_0 is the climate sensitivity parameter (for the Planck feedback alone), which equals 0.3 K W^{-1} m^{-2} at the reference state.

Greenhouse gas perturbations introduced by changing the optical depth τ_0 (ignoring possible feedbacks from S_0 and γ) lead to changes in LHF through changes in $(U - D)_{\mathrm{LCL}}$ (18). This can be expressed using (11) as

$$\Delta\mathrm{LHF} = (U - D)_{\mathrm{LCL}}\left(-\frac{\Delta\varepsilon_{\mathrm{LCL}}}{\varepsilon_{\mathrm{LCL}}} - \frac{4\Delta\theta}{\theta}\right). \tag{21}$$

The two terms in the parentheses on the rhs correspond to changes in two different aspects of the longwave radiative transfer, each of which depends on τ_0 in ways that depend in turn on the details of the radiative transfer. In particular, the second term indicates that warming is directly associated with a *decrease* in LHF because of the associated increase in $(U - D)_{\mathrm{LCL}}$. However, the strong reduction in $\varepsilon_{\mathrm{LCL}}$ with increasing τ_0 (Fig. 4) leads to a net increase in LHF. For instance, near the reference climate in the idealized model, the $\varepsilon_{\mathrm{LCL}}$ and the θ term account for 120% and −20% of the increase in LHF, respectively. This explains the relative insensitivity of the relation between τ_0 and LHF to the lapse rate reported in section 3, because $\varepsilon_{\mathrm{LCL}}$ is insensitive to Γ (Fig. 4), whereas θ itself depends strongly on Γ through $\varepsilon_{\mathrm{TOA}}$ (Fig. 4).

Considering both longwave and shortwave forcings at the TOA (ΔF_L and ΔF_S, respectively), the response in LHF in terms of the parameters of the system is given by

$$\Delta\mathrm{LHF} = \alpha_L(\tau_0)\Delta F_L + \alpha_S(\tau_0, \gamma)\Delta F_S - S_0\Delta\gamma, \tag{22}$$

where

$$\alpha_L \equiv \left(\frac{\partial\varepsilon_{\mathrm{LCL}}}{\partial\varepsilon_{\mathrm{TOA}}} - \frac{\varepsilon_{\mathrm{LCL}}}{\varepsilon_{\mathrm{TOA}}}\right) \quad \text{and} \tag{23}$$

$$\alpha_S \equiv \left(1 - \gamma - \frac{\varepsilon_{\mathrm{LCL}}}{\varepsilon_{\mathrm{TOA}}}\right) \tag{24}$$

are coefficients that depend only on τ_0 and γ and are generally different from each other (Fig. 6). The fact that $\varepsilon_{\mathrm{TOA}}$ is a monotonic (decreasing) function of τ_0 (Fig. 4) has been used to remove the explicit dependence on τ_0. This will prove useful in section 5 when dealing with a realistic radiative transfer model for

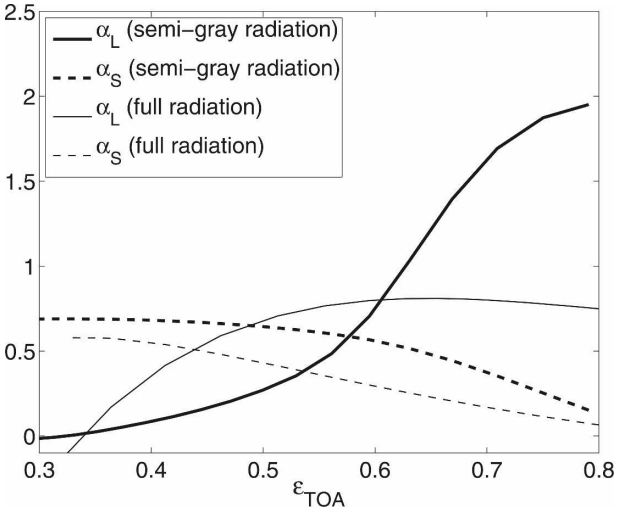

FIG. 6. Change in LHF per unit radiative perturbation associated with variations in τ_0 (α_L, solid) and S_0 (α_S, dashed), plotted against $\varepsilon_{\mathrm{TOA}}$ for semigray radiation (thick) and full radiation with interactive water vapor feedback (thin). The constant value $\gamma = 0.29$ is assumed throughout.

which τ_0 is not well defined. Because $\varepsilon_{\mathrm{TOA}}$, $\varepsilon_{\mathrm{LCL}}$ and γ are all positive, in general $\alpha_S \leq 1$. On the other hand, $\alpha_L < 1$ only for relatively high optical thickness (Fig. 6), at values of $\varepsilon_{\mathrm{TOA}}$ smaller than the reference value of around 0.6 (i.e., $\tau_0 > 6$).

In the special cases in which either only ΔF_L or ΔF_S is nonzero and $\Delta\gamma = 0$, (20) and (22) can be used to uniquely relate ΔLHF and $\Delta\theta$. In the more general case in which $\Delta F = \Delta F_L + \Delta F_S$, however, (20) and (22) yield

$$\Delta\mathrm{LHF} = \lambda_0^{-1}\left(\frac{\alpha_L + \alpha_S}{2}\right)\Delta\theta + \left(\frac{\alpha_L - \alpha_S}{2}\right)(\Delta F_L - \Delta F_S), \tag{25}$$

so only if $\alpha_L = \alpha_S$ would the relation between ΔLHF and $\Delta\theta$ be indifferent to the type of forcing in this model. However, because τ_0 in the real atmosphere is dominated by water vapor, which itself is a strong function of temperature, a pure shortwave forcing would also be associated with changes in the longwave transfer (i.e., τ_0). It will be shown in the next subsection that the presence of radiative feedbacks at the TOA merges these idealized responses as well.

The coefficient $\alpha_L(\tau_0)$, which determines the response of LHF to a pure longwave forcing, depends on the relation between $\varepsilon_{\mathrm{LCL}}$ and $\varepsilon_{\mathrm{TOA}}$, reflecting the opposing effects on $(U - D)_{\mathrm{LCL}}$ of surface warming and the reduction in longwave transmissivity noted previously. This coefficient (and hence the rate of increase of LHF) drops to low values as $\varepsilon_{\mathrm{TOA}}$ decreases (equivalently, as τ_0 increases; Fig. 6), as required by (19).

With respect to shortwave absorption, because γ does not enter (16) or (17) explicitly, it is a sort of wildcard that can be arbitrarily varied (e.g., by changing concentrations of atmospheric black aerosols) and consequently change LHF with no effect on the temperatures and other fluxes. As shown later, there are changes in γ in nature associated with changes in water vapor with warming that might have a significant effect on the changes in LHF.

b. Radiative feedbacks

So far, the longwave optical depth τ_0, the incoming insolation S_0, and the atmospheric shortwave absorptivity γ have been taken as external parameters of the system. On the earth, water vapor is the most important greenhouse gas and absorber of insolation in the troposphere and is strongly tied to the atmospheric temperature. Similarly, albedo, particularly the component associated with ice and clouds, is also affected by temperature.

For radiative purposes, climate models approximately maintain a constant free troposphere relative humidity (Soden and Held 2006), which implies that specific humidity increases with temperature following approximately the Clausius–Clapeyron (C–C) relation. The resulting positive radiative feedback is partly offset by the negative feedback associated with the reduction in the lapse rate Γ, which was shown previously to have a relatively weak direct effect on LHF, and it is the resulting net positive feedback that is robust among climate models (Soden and Held 2006). Thus, the radiative feedbacks from water vapor can be crudely incorporated into the present model by taking τ_0 and γ to be monotonically growing functions of θ. Similarly, a dependence of Γ on θ can also be assumed for calculating changes in $\varepsilon_{\mathrm{TOA}}$. On the other hand, the sign of the albedo feedback is less constrained, and we will just assume that an effect of temperature on albedo exists.

With this enhancement of the model, the semianalytical solution (16)–(18) remains adequate, but ε now depends on θ through τ_0. Given S_0 and the functional dependence of τ_0 on θ, (16) can be directly solved for θ and, therefore, for τ_0. This then determines δT and LHF through (17) and (18). The climate sensitivity with feedbacks is given by (16) as

$$\frac{\Delta\theta}{\Delta F} = \left(\frac{1}{1 - f_L - f_S}\right)\lambda_0 \equiv G\lambda_0, \tag{26}$$

where

$$f_L \equiv -\lambda_0\sigma\theta^4\left(\frac{\partial\varepsilon_{\mathrm{TOA}}}{\partial\tau_0}\frac{\partial\tau_0}{\partial\theta} + \frac{\partial\varepsilon_{\mathrm{TOA}}}{\partial\Gamma}\frac{\partial\Gamma}{\partial\theta}\right) \quad \text{and} \tag{27}$$

$$f_S \equiv \lambda_0\frac{\partial S_0}{\partial\theta} \tag{28}$$

are the longwave (e.g., water vapor, lapse rate) and shortwave (i.e., surface and cloud albedo) feedback parameters, respectively. The feedbacks enhance the response of θ to a radiative forcing by the gain factor G.

The changes in LHF are given by

$$\Delta\text{LHF} = G[(1 - f_S)\alpha_L + f_S\alpha_S]\Delta F_L + G[(1 - f_L)\alpha_S + f_L\alpha_L]\Delta F_S - S_0\Delta\gamma. \quad (29)$$

The radiative feedbacks lead to an amplification of the response of LHF to the forcings by the gain factor G. Because the response in θ is amplified by the same factor, this does not alter the ratio of the changes in LHF and θ under pure longwave or shortwave forcing. However, the presence of shortwave (longwave) feedbacks also leads to the combination of α_L and α_S into an effective coefficient in the case of a pure longwave or shortwave forcing. In the case of positive feedbacks, the effective coefficients lie between α_L and α_S.

c. *Effect of changes in p_{LCL}*

As noted before, besides its role as a greenhouse gas, the low level water vapor affects the equilibrium climate state through its effect on p_{LCL}, which was kept constant in the idealized model for simplicity. This effect is not large enough to change the qualitative behavior of the system (cf. the experiments with fixed Γ but with p_{LCL} fixed and interactive in Fig. 2), but is not negligible.

From the definition of the LCL, we have

$$\frac{\Delta p_{\text{LCL}}}{p_{\text{LCL}}} \approx \left(\frac{R_d L_v}{c_p R_v T_{\text{LCL}}} - 1\right)^{-1}\left[\frac{\Delta q}{q} - \frac{\theta}{T_{\text{LCL}}}\frac{L_v\Delta\theta}{R_v\theta^2}\right], \quad (30)$$

where $T_{\text{LCL}} = \theta \times (p_{\text{LCL}}/p_0)^{R_d/c_p}$. Whereas moistening is associated with an increase in p_{LCL}, warming has an opposing effect. This net result of this cancelation is seen more clearly by writing the second term on the rhs of (30) in terms of the surface relative humidity r_0 as

$$\left[\frac{\Delta r_0}{r_0} + \left(1 - \frac{\theta}{T_{\text{LCL}}}\right)\frac{L_v}{R_v\theta^2}\Delta\theta\right]. \quad (31)$$

For typical values, the coefficient of the $\Delta\theta$ term is around $-0.2\%\ \text{K}^{-1}$. On the other hand, the ratio $(\Delta r_0/r_0)/\Delta\theta$ can have larger magnitudes and the first term in (31) generally dominates, but its value varies significantly under greenhouse forcing. For instance, in the full radiative–convective model, the values range from -1.1% to $1.7\%\ \text{K}^{-1}$ at temperatures below and above the reference, respectively.

Increasing p_{LCL} modifies slightly the atmospheric thermal structure and therefore the ε profile, but this effect is small compared to the reduction in ε_{LCL} associated with the downward displacement of the LCL along the unperturbed ε profile, which decreases with increasing p (Fig. 3). Therefore, (18) predicts that if p_{LCL} increases, the LW fluxes at the LCL would decrease and lead to an increase in LHF. Whether this effect enhances or reduces the increase in LHF with increased τ_0 or S_0 will depend on whether r_0 increases or decreases, respectively.

Including the latter effect of the changes in p_{LCL} on LHF results in the addition of the term

$$-\sigma\theta^4\left.\frac{\partial\varepsilon}{\partial p}\right|_{p_{\text{LCL}}}\Delta p_{\text{LCL}} \quad (32)$$

to the rhs of (29), which can be expressed in terms of q and θ using (30). In principle, the resulting equation can be solved for ΔLHF similarly to (29), but the complexity of the resulting formula is such that it does not provide clear insights. An empirical approach will be used in the next subsection.

d. *Effect of changes in C*

If C were increased (e.g., by increasing surface wind speed), the instantaneous response in LHF would be a proportional increase. However, once equilibrium is regained, the radiative constraints will prevail, so there will be an adjustment in T_s and q that will significantly alter this response (BR89). As indicated in section 4, the adjustment of q to a change in C could be such that LHF remains unchanged. However, as shown in the previous subsection, q itself affects the longwave fluxes at the LCL by affecting p_{LCL}, which in turn controls LHF. Thus, in equilibrium, changes in C can result in changes in LHF, but the magnitude of this change will be largely constrained by radiative considerations.

In the general case, C can be expected to respond to changes in climate, and the simplest assumption is that ΔC is linearly related to $\Delta\theta$. To assess the effect of ΔC on the ΔLHF associated with greenhouse forcing, rather than assuming specific relationships between ΔC and $\Delta\theta$, a number of scenarios with different prescribed increases in C but the same increase in τ_0 are compared to a control case. The two approaches are equivalent for the equilibrium results but the latter is simpler to implement. Thus, the full radiative–convective model (with interactive p_{LCL} and pseudoadiabatic lapse rate) was run with a perturbation in τ_0 and various perturbations in C. The results indicate that a fractional change in C per degree warming of about $5\%\ \text{K}^{-1}$ results in an enhancement in the increase in LHF with the warming of around $1\%\ \text{K}^{-1}$, relative to the change in

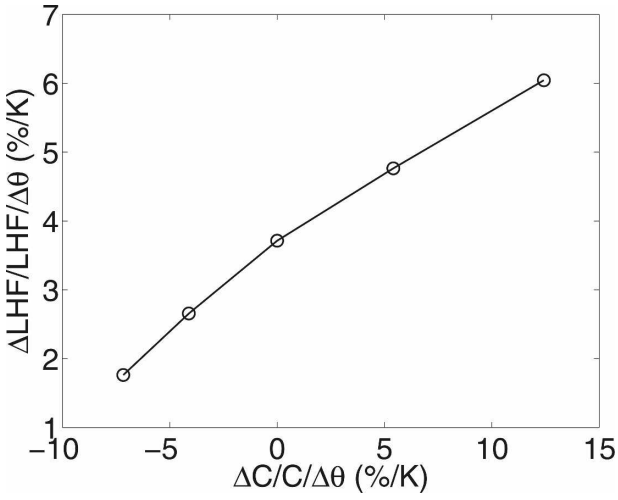

FIG. 7. Fractional changes in LHF per degree warming (% K^{-1}) for different changes in C (% K^{-1}).

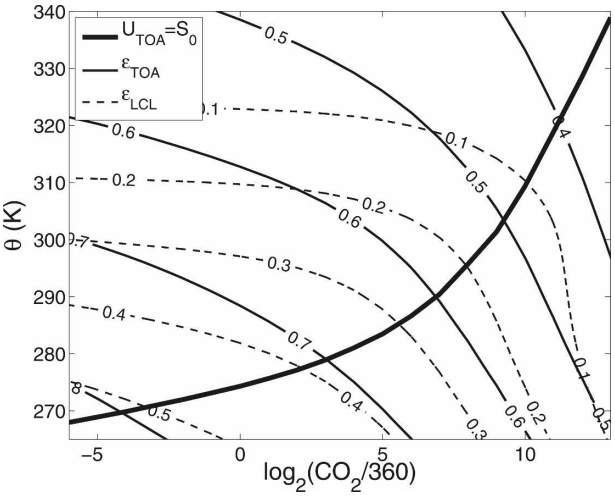

FIG. 8. Contours of $\varepsilon_{\mathrm{TOA}}$ (solid) and $\varepsilon_{\mathrm{LCL}}$ (dashed) as CO_2 concentration and water vapor are varied (the latter by changing θ while keeping relative humidity constant). The thick curve denotes the states for which $U_{\mathrm{TOA}} = S_0 = 240$ W m^{-2}.

the case in which $\Delta C = 0$ (about 3.7% K^{-1}; Fig. 7). Thus, the equilibrium effect of changes in C on LHF is about a factor of 4–5 smaller than would be expected from the instantaneous response. This is even more dramatic in the model of BR89 (which is similar to the present one but with more comprehensive physics), in which the fractional increase in LHF is 10–20 times smaller than the fractional increase in C (their Fig. 19). In the present model, around 80% of the effect of ΔC on ΔLHF is associated, through $(U - D)_{\mathrm{LCL}}$ (21), with the change in p_{LCL} and the rest is associated with the change in $\sigma\theta^4$ (note that $\Delta\theta$ is not the same for the different ΔC because of the differences in lapse rate and p_{LCL}).

5. Full radiative transfer

To assess how the behavior of the semianalytical model (16)–(18) from section 4 changes when the semigray radiation scheme is replaced with a realistic radiative transfer model, the National Center for Atmospheric Research (NCAR) Column Radiation Model, based on the physics of the NCAR Community Climate Model version 3 (CCM3) climate model (Kiehl et al. 1996), was used for the radiative calculations in this section. No greenhouse gases besides CO_2 and water vapor were considered. Conceptually, this case is not as straightforward as with the semigray radiation because the effective τ_0 has both an externally prescribed component due to CO_2 and a component that depends on θ itself due to water vapor (cf. section 4b) and, in fact, τ_0 is not well defined in this case. However, the assumption about relative humidity described next provides the additional constraint necessary for overcoming this difficulty.

The ε profiles were calculated with this radiation model as in section 4 [i.e., taking $\delta T = 0$ and $\varepsilon \equiv (U - D)/\sigma\theta^4$; see Eq. (9)] for different values of θ and CO_2 concentrations, using the same Γ and p_{LCL} as in the semianalytic model, but with the humidity distribution determined by prescribing the vertical profile of relative humidity r from Manabe and Wetherald (1967):

$$r = \begin{cases} 0.77\dfrac{p/p_0 - 0.02}{1 - 0.02}, & \text{for } p/p_0 > 0.02, \\ 0, & \text{otherwise.} \end{cases} \tag{33}$$

The fixed relative humidity assumption is a good approximation for the longwave radiative effects of water vapor in climate models (Soden and Held 2006). Note that the relative humidity distribution (33) was used for the radiative calculations only; at the surface, the relative humidity (r_0) remained interactive for the calculations associated with LHF.

The CO_2 concentration was varied between 2^{-6} and 2^{13} times a representative value of 360 ppm. For each concentration, the value of θ consistent with $U_{\mathrm{TOA}} = S_0 = 240$ W m^{-2}, was determined (Fig. 8). A transition between these climate states can be qualitatively interpreted as an equilibrium climate change associated with an external perturbation (e.g., anthropogenic) in CO_2.

a. Response to CO_2 perturbations

Because τ_0 is not well defined outside of the semigray radiation context, the results are presented in terms of

$\varepsilon_{\mathrm{TOA}}$, which monotonically decreases as greenhouse gases are added to the atmosphere. This approximation assumes that different greenhouse gases change the ε profiles in the same way—particularly, that changes in $\varepsilon_{\mathrm{TOA}}$ are associated with unique changes in $\varepsilon_{\mathrm{LCL}}$ and $\varepsilon_{\mathrm{sfc}}$ independently of what greenhouse gases are perturbed. This is not expected a priori to be an accurate approximation because different greenhouse gases have different vertical distributions and absorption properties, but the results indicate that it is adequate because the variations in CO_2 and water vapor have similar effects on $\varepsilon_{\mathrm{LCL}}$ relative to $\varepsilon_{\mathrm{TOA}}$ (the isolines are roughly parallel in Fig. 8). This approximation is particularly good around the states for which $S_0 = 240$ W m^{-2} (thick line in Fig. 8) but is inadequate at low CO_2 concentrations and high water vapor (low CO_2 and high θ in Fig. 8), at which $\varepsilon_{\mathrm{LCL}}$ is insensitive to CO_2 but not to water vapor, probably reflecting the vertical distribution of the latter, which allows it to prevail in the lower troposphere.

The values of α_L and α_S were estimated for the climates with $U_{\mathrm{TOA}} = S_0 = 240$ W m^{-2} (Fig. 6). The results for α_S are qualitatively similar to the semigray radiation case, but α_L shows significant differences. In particular, the values of α_L do not present the large variations observed with the semigray radiation and remain between 0.6 and 0.8, except for CO_2 concentrations greater than 2^8 times the reference, above which the values drop (Fig. 6). Thus, for a large range of perturbations in CO_2 concentrations, α_L is approximately uniform and consistently smaller than unity, and LHF behaves rather linearly in this regime (Fig. 5). This behavior is associated with the fact that as CO_2 (and water vapor) is increased, the ε profile is rather uniformly shifted to lower values (Fig. 9), so $\partial\varepsilon_{\mathrm{LCL}}/\partial\varepsilon_{\mathrm{TOA}}$ is close to unity, in contrast to the strong deformation in the profiles observed in the case of the semigray radiation (Fig. 3), which results in $\partial\varepsilon_{\mathrm{LCL}}/\partial\varepsilon_{\mathrm{TOA}}$ larger than unity at low values of τ_0.

Near the reference climate ($\varepsilon_{\mathrm{TOA}} \sim 0.6$), the coefficients α_L and α_S take values of 0.8 and 0.3, respectively (Fig. 6). The value for f_S is taken as approximately 0.2, based on the analysis of cloud and surface albedo shortwave feedbacks from climate models by Colman (2003). Therefore, $[(1 - f_S)\alpha_L + f_S\alpha_S] \approx 0.7$ and, with $\lambda_0^{-1} = 3.21$ W m^{-2} K^{-1} [the mean of the values from various climate models reported by Soden and Held (2006)], (26) and (29) predict that the ratio of the responses in LHF and θ to a pure CO_2 perturbation with fixed γ is $\Delta\mathrm{LHF}/\Delta\theta \approx 2.2$ W m^{-2} K^{-1}. This is comparable to the results from comprehensive climate models (HS06), but the concomitant increase in atmospheric shortwave absorption results in a smaller rate of increase in LHF (Takahashi 2008, manuscript submitted to *J. Climate*, hereafter T08), as illustrated next.

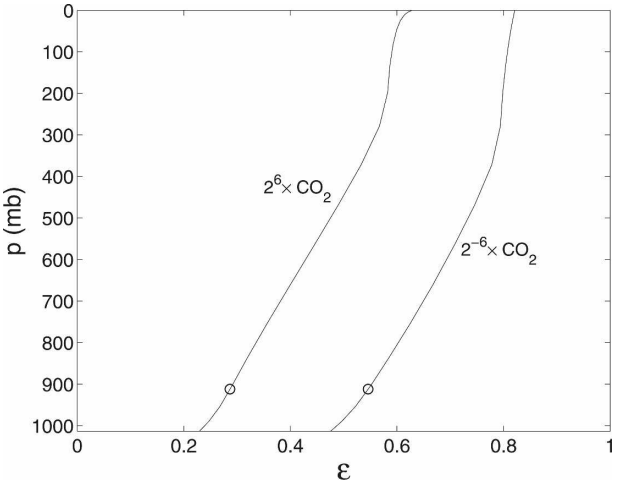

FIG. 9. Similar to Fig. 3, but using the full radiative transfer model for 2^{-6} and 2^6 times the reference CO_2 concentration (360 ppm) and the corresponding values of θ consistent with $U_{\mathrm{TOA}} = 240$ W m^{-2}.

b. Changes in shortwave absorption

To estimate the changes in absorption of shortwave radiation in the clear sky atmosphere, the full-radiation calculations were made with equinoctial insolation at a solar zenith angle of 38.3° (the average at the equator; Hartmann 1994) at a tropical latitude of 15°, using no radiatively active gases except water vapor and CO_2.

The increase in the fraction γ of absorbed shortwave radiation (calculated as the ratio of the surface to the TOA net shortwave fluxes)[2] resulting directly from quadrupling the concentration of CO_2 is comparable to the increase associated with the increase in water vapor due to a warming of 0.2 K (Fig. 10), which is small compared to the warming of more than 4 K expected for that forcing, based on a variety of comprehensive climate models (Randall et al. 2007). The reduction in CO_2 concentration by a factor of 4 has a larger direct effect than its increase (Fig. 10), but it is still small compared to the water vapor effect.

The water vapor dependence of γ is linear on θ for fixed relative humidity (Fig. 10) with a slope of $\Delta\gamma/\Delta\theta \sim 0.23\%$ K^{-1}. Although the atmosphere is optically thin for shortwave radiation, γ increases with θ considerably more slowly than C–C suggests. This is probably because the relevant water vapor absorption bands (in the

[2] The contribution of the subcloud layer to γ and its variation with θ is an order of magnitude smaller.

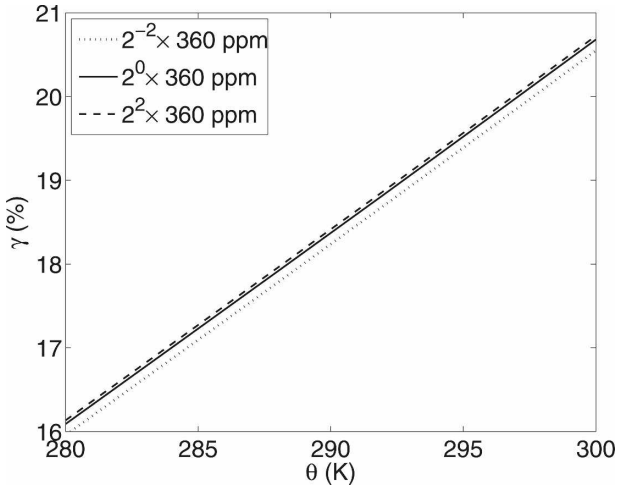

FIG. 10. Fraction (γ, in percent) of net shortwave at the TOA absorbed in the atmosphere as a function of the water vapor distribution (obtained from a fixed relative humidity profile and different values of θ) and for three concentrations of CO_2.

near-infrared) are already close to saturation, and therefore the atmosphere is not optically thin at those frequencies.

With $S_0 = 240$ W m^{-2}, (29) indicates that the increase in clear sky shortwave absorption by water vapor should lead to a reduction in the rate of increase of LHF with respect to θ by about 0.5 W m^{-2}K^{-1} (i.e., from 2.2 to 1.7 W m^{-2} K^{-1}). The γ effect estimated in this study is relatively small, but in some comprehensive climate models it is comparable to the LHF change (T08).

6. Discussion

The simplest version of the radiative–convective equilibrium model considered in this study has three unknowns: the surface air temperature, the sea–air temperature difference and the surface latent heat flux. The first of these is solved for from the energy balance at the top of the atmosphere, as in the original versions of the radiative–convective models in which this was the only variable (see review by Ramanathan and Coakley 1978). In these models, the total convective vertical energy flux could be diagnosed by requiring it to balance the radiative cooling associated with the prescribed convectively neutral lapse rate. The partitioning of this flux between the different components at the surface could not be determined because it involves at least one additional variable and therefore requires one more equation. This extra constraint is provided in the present model by considering the energy budget of the subcloud layer. The additional information is then provided by the vertical structure of the longwave fluxes and its magnitude at cloud base, which can be calculated based on the surface temperature and the greenhouse gas distribution, allowing the latent heat flux plus the atmospheric shortwave absorption to be determined, as well as the sea–air temperature difference. The role of low-level moisture in the solution is indirect and is manifested mainly through its influence on the pressure at the LCL, which is mainly affected by relative humidity, and on the lapse rate in the free troposphere, which affects primarily the surface air temperature.

Another apparently reasonable closure that has been used in similar models is setting the surface relative humidity r_0 to a fixed value (e.g., Lindzen et al. 1982; Pierrehumbert 2002), which is motivated by the weak observed variability in r_0. The constant relative humidity approximation is indeed adequate for explaining the changes in the water content of the atmosphere (HS06) with temperature because the rate of increase in the saturation specific humidity with temperature, which follows the Clausius–Clapeyron scaling, is large ($\sim$7% K^{-1}) compared to the changes in relative humidity. However, surface evaporation is more sensitive to changes in r_0 than moisture content because it depends approximately on $q_s(T_s)(1 - r_0)$. Thus, for $r_0 \approx 0.8$, a modest fractional change in r_0 of 1% per degree warming would be translated into a larger change in evaporation (-4%), which would significantly offset the $\sim$7% associated with the C–C increase in q_s. For this reason, the models or observational estimates (e.g., Wentz et al. 2007) that assume constant r_0 tend to produce increases in LHF that essentially follow C–C scaling, whereas models that predict r_0 (e.g., BR89 and the present study) have changes in LHF largely unrelated to C–C.

The fact that changes in LHF relative to temperature are only weakly related to changes in moisture implies that the residence time of moisture will generally also change. Comprehensive models for climates close to the present have an increase in LHF weaker than C–C associated with greenhouse forcing, so the residence time increases. This has been interpreted as a weakening of the motions responsible of transporting the moisture vertically (BR89; Betts 1998; HS06; Vecchi and Soden 2007). The present model does not explicitly consider vertical motions and no assumption has been made relating any such motion to the moisture budget, so it predicts the change in the residence time with no reference to dynamical processes. Furthermore, the relation between the strength of the vertical motions and the moisture transport might not be straightforward. For instance, explicitly writing the vertical moisture

transport flux as $\langle M'q' \rangle$, where M is the vertical mass flux, $\langle \cdot \rangle$ indicates a global average, and primes indicate deviation from it (note that $\langle M \rangle = 0$ in equilibrium), allows its fractional changes to be written as

$$\frac{\Delta\langle M'q' \rangle}{\langle M'q' \rangle} = \frac{\Delta\sqrt{\langle M'^2 \rangle}}{\sqrt{\langle M'^2 \rangle}} + \frac{\Delta\sqrt{\langle q'^2 \rangle}}{\sqrt{\langle q'^2 \rangle}} + \frac{\Delta\rho}{\rho}, \quad (34)$$

where

$$\rho = \frac{\langle M'q' \rangle}{\sqrt{\langle M'^2 \rangle}\sqrt{\langle q'^2 \rangle}} \quad (35)$$

is the spatial correlation coefficient between M and q. Thus, assuming the changes in the moisture flux and the moisture fluctuations as given, either the strength of the vertical motions (represented by the standard deviation of M) or the correlation ρ could adjust to satisfy (34). Preliminary experiments with a GCM in radiative–convective equilibrium with no convective parameterization (i.e., moist convection takes place in the resolved scales) suggest that changes in ρ can be as important as those in the strength of M in (34). In full GCMs, however, the changes in ρ are not as important when considering the parameterized convective mass fluxes or the resolved zonally asymmetric tropical overturning (Vecchi and Soden 2007). The former is probably due to the way the convective schemes are constructed (i.e., ρ might be prescribed to some extent), while the latter is perhaps associated with geographical constraints on the pattern of both the circulation and moisture distribution that do not exist in the radiative–convective setting. These matters deserve further study.

The results with the full radiative transfer model (section 5) are in quantitative agreement with those from comprehensive climate models, but because there was no a priori expectation that the present model would behave similarly to a global climate model, it is possible that this agreement is fortuitous. However, OS07 indicated that a radiative–convective version of their semigray radiation GCM provided a good representation of the latter under a broad range of forcings, suggesting that the earth might approximately behave as a radiative–convective equilibrium model regarding the global hydrological cycle. The question then arises of what are the fundamental differences between the global energy budgets of a radiative–convective world and a rotating planet with differential heating. If the global mean vertically varying energy equation were obtained for the latter, a few terms involving spatial covariances would appear that are not in the present radiative–convective model. One of these terms is the vertical transport of dry static energy by the large-scale circulation, but, as mentioned in the introduction, this term is small (less than 10 W m^{-2} globally) compared to the latent heat flux. Another one is associated with the logarithmic dependence of U_{TOA} on specific humidity, which implies that spatial variations in the latter can have significant effects on the spatial mean of the former (Pierrehumbert et al. 2006). The relevance of the present model to the global mean hydrological cycle is therefore contingent upon the relative smallness of these covariance terms.

The effects of clouds on the hydrological cycle were not considered in the present model. Although the associated feedbacks at the TOA are considered in (26) and (29), changes in clouds can potentially also affect the α_L coefficient (23) by modifying the shape of the vertical profile of the longwave fluxes. This remains to be addressed, although the fact that comprehensive climate models under greenhouse forcing show robust changes in LHF plus atmospheric absorption of shortwave (T08), despite significant differences in the treatment of clouds, suggests that this effect is probably small, at least in current climate models.

7. Summary and conclusions

A one-dimensional radiative–convective equilibrium model has been formulated in terms of the energy budgets at the top of the atmosphere, the free atmosphere, and the subcloud layer. The surface relative humidity and the air–sea temperature difference are part of the solution. Using semigray radiative transfer and prescribing the pressure at the LCL and the free atmospheric lapse rate (which does not qualitatively change the behavior of the system), semianalytical solutions for surface air temperature, the sea–air temperature difference, and the surface latent heat flux (LHF) are obtained in terms of the radiative properties of the system alone (i.e., longwave optical depth, shortwave absorptivity, net incoming shortwave). This solution then allows the surface humidity to be diagnosed for a given wind speed and other parameters controlling the surface moisture flux.

The semianalytical solution shows that forcing through increased greenhouse gases leads to an increase in LHF through a reduction in the net longwave flux through the LCL due to the increased opacity of the low-level atmosphere, despite an opposing direct effect from the increased surface air temperature, which enhances the longwave flux at the LCL. On the other hand, the same change in the longwave flux through the LCL is associated with a decrease in the longwave cooling in the subcloud layer, so a reduction

in the sea–air temperature difference is required to reduce the surface longwave and sensible heat fluxes and maintain the energy balance in this layer.

In the simplest version of the model, the rate of increase in LHF relative to θ under greenhouse forcing is given by $\Delta\mathrm{LHF}/\Delta\theta \approx \lambda_0^{-1}\alpha_L$, where $\lambda_0^{-1} \approx 3.2\ \mathrm{W\ m^{-2}/K}$ is the Planck feedback and α_L is a coefficient that depends only on the relative magnitudes of the net longwave fluxes at the LCL and the TOA. When a full radiative transfer model with an interactive water vapor longwave radiative effect (assuming fixed relative humidity for radiative purposes only), α_L took a value of around 0.8, which leads to $\Delta\mathrm{LHF}/\Delta\theta \approx 2.6\ \mathrm{W\ m^{-2}\ K^{-1}}$ under greenhouse forcing. Radiative feedbacks modify the effective coefficient and, using an estimate of shortwave feedbacks, the effective coefficient and the change in LHF are reduced to 0.7 and 2.2 $\mathrm{W\ m^{-2}\ K^{-1}}$, respectively. The increase in clear-sky shortwave absorption associated with the increase in water vapor reduces the latter further to 1.7 $\mathrm{W\ m^{-2}\ K^{-1}}$, close to what comprehensive climate models predict for the global hydrological cycle (HS06).

The prescription of the pressure at the LCL (p_{LCL}) and the lapse rate in the free atmosphere makes LHF insensitive to the specific humidity at the surface, so the Clausius–Clapeyron relation has no bearing on LHF in this case. More generally, p_{LCL} is sensitive to the surface relative humidity r_0. However, in the case of greenhouse forcing, increases in temperature and moisture have opposing effects on r_0 and the resulting effect on LHF through p_{LCL} is subtle. On the other hand, a change in wind speed leads to a more robust increase in r_0, so p_{LCL} is increased, which results in a decrease in the longwave flux at the LCL and, therefore, in an increase in LHF. However, at most 25% of the relative change in wind speed translates into a change in LHF.

Acknowledgments. The author thanks Drs. Isaac M. Held and Gabriel A. Vecchi for useful discussions and Drs. Held and Geoffrey K. Vallis for comments on the manuscript. Discussions with Drs. L. E. Back, D. S. Battisti, P. Caldwell, D. M. W. Frierson, P. A. O'Gorman, O. M. Pauluis, G. Roe, and M. Zhao, as well as the comments from two anonymous reviewers, are also appreciated. This research was supported by the National Oceanic and Atmospheric Administration (NOAA) Climate and Global Change Postdoctoral Fellowship Program, administered by the University Corporation for Atmospheric Research, under Award NA06OAR4310119 from the NOAA Climate Programs Office, U.S. Department of Commerce, with additional funding from Award NA17RJ2612 from NOAA, U.S. Department of Commerce. The author thanks the NOAA Geophysical Fluid Dynamics Laboratory for hosting him during the development of this study. The statements, finding, conclusions, and recommendations are those of the author and do not necessarily reflect the views of the NOAA Climate Program Office or the U.S. Department of Commerce.

REFERENCES

Allen, M. R., and W. J. Ingram, 2002: Constraints on future changes in climate and the hydrologic cycle. *Nature,* **419,** 224–232.

Betts, A. K., 1973: Non-precipitating cumulus convection and its parameterization. *Quart. J. Roy. Meteor. Soc.,* **99,** 178–196.

——, 1998: Climate–convection feedbacks: Some further issues. *Climatic Change,* **39,** 35–38.

——, and W. Ridgway, 1989: Climatic equilibrium of the atmospheric convective boundary layer over a tropical ocean. *J. Atmos. Sci.,* **46,** 2621–2641.

Colman, R., 2003: A comparison of climate feedbacks in general circulation models. *Climate Dyn.,* **20,** 865–873.

Frierson, D. M. W., I. M. Held, and P. Zurita-Gotor, 2006: A gray-radiation aquaplanet moist GCM. Part I: Static stability and eddy scale. *J. Atmos. Sci.,* **63,** 2548–2566.

Goody, R. M., and Y. L. Yung, 1989: *Atmospheric Radiation: Theoretical Basis.* 2nd ed. Oxford University Press, 519 pp.

Hartmann, D. L., 1994: *Global Physical Climatology.* Academic Press, 411 pp.

Held, I. M., and B. J. Soden, 2006: Robust responses of the hydrological cycle to global warming. *J. Climate,* **19,** 5686–5699.

Kiehl, J. T., J. J. Hack, G. B. Bonan, B. A. Boville, B. P. Briegleb, D. L. Williamson, and P. J. Rasch, 1996: Description of the NCAR Community Climate Model (CCM3). NCAR Tech. Note NCAR/TN-420+STR, 152 pp.

Larson, K., D. L. Hartmann, and S. A. Klein, 1999: The role of clouds, water vapor, circulation, and boundary layer structure in the sensitivity of the tropical climate. *J. Climate,* **12,** 2359–2374.

Lindzen, R. S., A. Y. Hou, and B. F. Farrell, 1982: The role of convective model choice in calculating the climate impact of doubling CO_2. *J. Atmos. Sci.,* **39,** 1189–1205.

Manabe, S., and R. F. Strickler, 1964: Thermal equilibrium of the atmosphere with a convective adjustment. *J. Atmos. Sci.,* **21,** 361–385.

——, and R. T. Wetherald, 1967: Thermal equilibrium of the atmosphere with a given distribution of relative humidity. *J. Atmos. Sci.,* **24,** 241–258.

O'Gorman, P. A., and Schneider, T., 2007: The hydrological cycle over a wide range of climates simulated with an idealized GCM. *J. Climate,* **21,** 3815–3832.

Pierrehumbert, R. T., 1995: Thermostats, radiator fins, and the local runaway greenhouse. *J. Atmos. Sci.,* **52,** 1784–1806.

——, 2002: The hydrologic cycle in deep-time climate problems. *Nature,* **419,** 191–198.

——, H. Brogniez, and R. Roca, 2006: On the relative humidity of the atmosphere. *The Global Circulation of the Atmosphere,* T. Schneider and A. H. Sobel, Eds., Princeton University Press, 143–185.

Ramanathan, V., and J. A. Coakley, 1978: Climate modeling

through radiative–convective models. *Rev. Geophys.,* **16,** 465–489.

Randall, D. A., and Coauthors, 2007: Climate models and their evaluation. *Climate Change 2007: The Physical Science Basis,* S. Solomon et al., Eds., Cambridge University Press, 589–662.

Sarachik, E. S., 1978: Tropical sea surface temperature: An interactive one-dimensional atmosphere–ocean model. *Dyn. Atmos. Oceans,* **2,** 455–469.

Soden, B. J., and I. M. Held, 2006: An assessment of climate feedbacks in coupled ocean–atmosphere models. *J. Climate,* **19,** 3354–3360.

Takahashi, K., 2008: The global hydrological cycle and atmospheric shortwave absorption in climate models under CO_2 forcing. *J. Climate,* submitted.

Vecchi, G. A., and B. J. Soden, 2007: Global warming and the weakening of the tropical circulation. *J. Climate,* **20,** 4316–4340.

Weaver, C. P., and V. Ramanathan, 1995: Deductions from a simple climate model: Factors governing surface temperature and atmospheric thermal structure. *J. Geophys. Res.,* **100** (D6), 11 585–11 591.

Wentz, F. J., L. Ricciardulli, K. Hilburn, and C. Mears, 2007: How much more rain will global warming bring? *Science,* **317,** 233–235.